

Sintering and Compaction of Powdered Materials

Tristan Wolff Schwab

March 19, Spring 2022

1 Introduction

Sintering is a manufacturing process in which objects are formed by fusing fine particulates together. Sintering can be used to form objects from materials such as powdered metals, ceramics, glasses, and advanced materials such as graphite and diamond. In special cases, the sintering process can be used in conjunction with compaction, a process in which finely ground stock material is pressed, to achieve desired material properties.

The process of compaction and sintering is generally more expensive than conventional methods (such as casting or machining) and as a result, industry demands to make the process cheaper for expansion into other industries. In this report, the author discusses encoding a numerical model to simulate the spark sintering process combined with compaction ³ to predict the optimal processing parameters to reach complete solidification in a certain time. An optimization algorithm is developed to characterize the optimal conditions given certain process constraints.

The parameters which are determined through the optimization are then re-evaluated to assess the improvement without optimization. This report models the interaction of mechanical compression, electrical (joule) heating, and pore collapse in the material being processed. Future applications of this report extend into other advanced manufacturing processes in which the material being processed is subject to a variety of complex processes which cannot be experimentally determined cost-effectively.

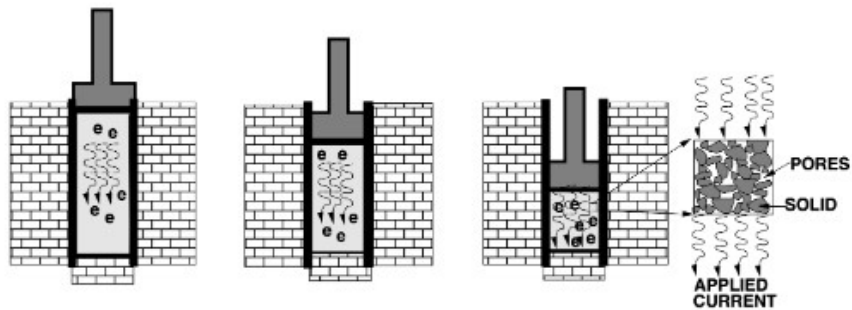


Figure 1: Compaction of powdered material with simultaneous applied current.

2 Methodology

Forward Euler Process Simulation

To simulate the process discussed, a Forward-Euler method was employed to solve a governing rate of thermal energy storage (see 10) on a single material point in one second using a time step of 10^4 . We started by building off the classical Kirchhoff-St. Venant constitutive relation for simple elasto-thermo-plastic decomposition of the total strain.

$$S = IE : (E - E_p - E_\theta) \quad (1)$$

where E represents the Green-Lagrange Strain, E_p represents the plastic strain, and E_θ represents the thermal strain. The process requires a thermodynamic foundation involving both mechanical and electrical energy conversion into heat. By the First Law of Thermodynamics:

$$\rho\dot{\omega} - S : \dot{E} + \nabla_X \cdot q_0 - \mathcal{J}H = 0 \quad (2)$$

where H is the rate of electromagnetic energy absorbed due to joule-heating in the current configuration. The model would be incomplete without consideration of both densification (the process in which the pores between particulates collapse) and the evolution of plastic strain. Under these considerations, the Elasticity Tensor IE , Electrical conductivity σ_c , densification stress threshold σ_d and yield strength, σ_y can be written by the following empirically-fit approximations:

$$IE = (1 - d)IE_0 e^{-P1 \frac{\theta - \theta_0}{\theta_0}} \quad (3)$$

$$\sigma_c = (1 - d)\sigma_{c0} e^{-P2 \frac{\theta - \theta_0}{\theta_0}} \quad (4)$$

$$\sigma_d = \sigma_{d0} e^{-P3 \frac{\theta - \theta_0}{\theta_0}} \quad (5)$$

$$\sigma_y = \sigma_{y0} e^{-P4 \frac{\theta - \theta_0}{\theta_0}} \quad (6)$$

where the constants $P1, P2, P3, P4$ are provided and d represents the densification parameter¹. After importing the relevant material constants and equations above, an elasticity tensor is constructed through the relation:

$$E_e = E - E_p - E_\theta \quad (7)$$

The Cauchy-Stress tensor is determined by the following equation:

$$\sigma = \frac{1}{J} F S F' \quad (8)$$

The deviatoric stress is determined by the following relation:

$$\sigma' = \sigma - \frac{1}{3} tr(\sigma) \quad (9)$$

The equations are then combined to solve an equation for the governing rate of thermal energy storage:

$$\dot{\theta} = \frac{S : \dot{E}_p + \frac{d}{2} e^{-P2 \frac{\theta - \theta_0}{\theta_0}} E_e : IE_0 : E_e - \nabla X \dot{q}_0 + \mathcal{J}H}{\rho_0 C - \beta tr(S) - \frac{(1-d)}{2\theta_0} P_1 e^{P1 \frac{\theta - \theta_0}{\theta_0}} E_e : IE_0 : E_e} \quad (10)$$

Genetic Algorithm Process Optimization

A genetic algorithm was used to identify the ideal process parameters aimed at minimizing the difference between a maximum temperature and a given desired temperature *and* identifying the final densification parameter (to ensure that the material is fully dense at some point before the end of the process). The initial densification parameter and the magnitude of the current density were generated random values subject to the following constraints:

- $0.5 \leq d(t = 0) \leq 0.9$
- $0 \leq J \leq 10^7$

The best children from Λ_d, Λ_J were sorted into separate structures before running through the process simulation. The maximum temperature and final densification parameter were returned and used to re-evaluate the cost function. The cost function implemented in this study was the following:

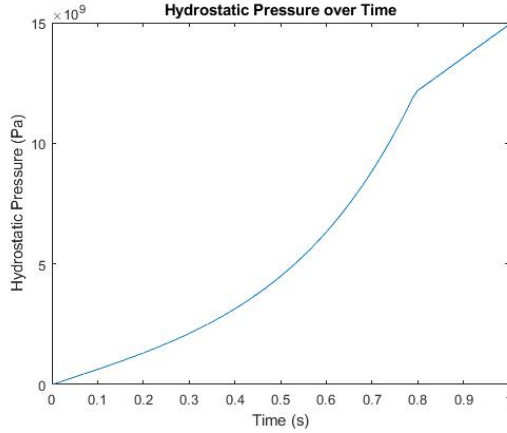
$$\Pi(\Lambda) = \omega_1 \left(\frac{\theta_{max} - \theta_{desired}}{\theta_{desired}} \right)^2 + \omega_2 d(t = t_f) \quad (11)$$

¹The densification and plasticity models used in this study can be found in the Appendix.

3 Results and Discussion

Process Simulation Analysis

The results from the Process Simulation are shown below. We expect an exponential increase of the hydrostatic pressure before densification occurs, which is well illustrated in the below figure, with densification occurring at roughly 0.8 seconds.



The magnitude of the deviatoric stress (recall, that deviatoric stress is the difference between the cauchy stress tensor and the hydrostatic pressure) decreases linearly throughout compression until complete solidification, at which point there is a large drop in the magnitude of σ' . A possible explanation may be that upon complete solidification, the same magnitude of compressive force has a small affect on stresses within the solid material.

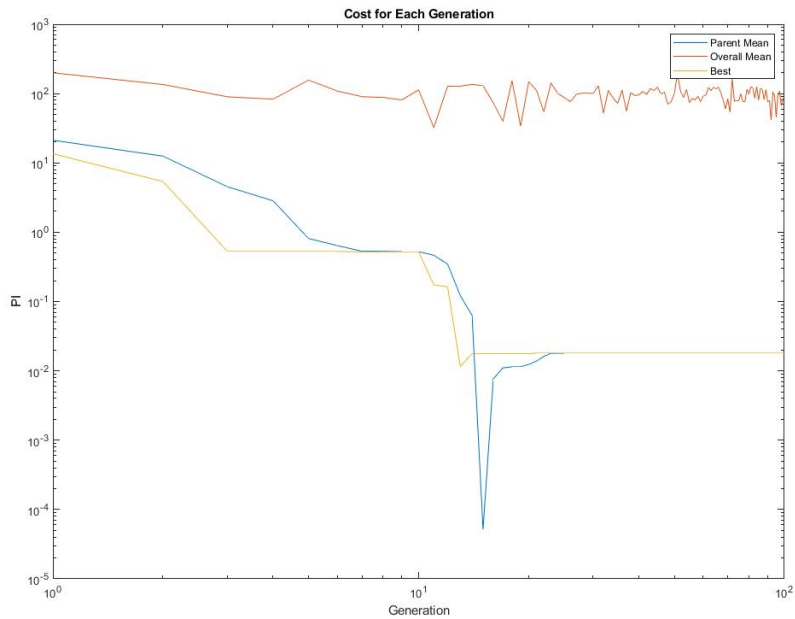
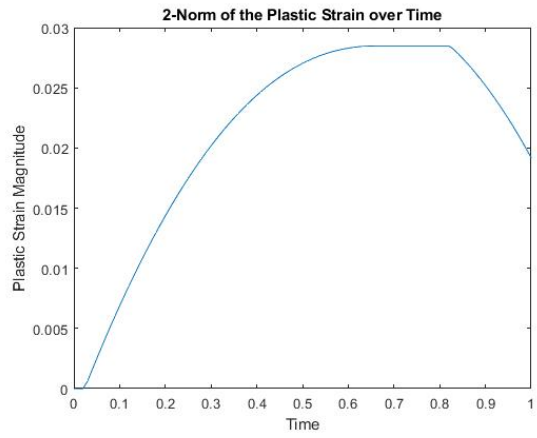
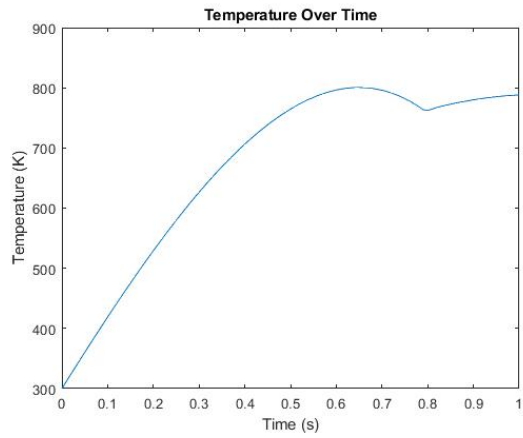
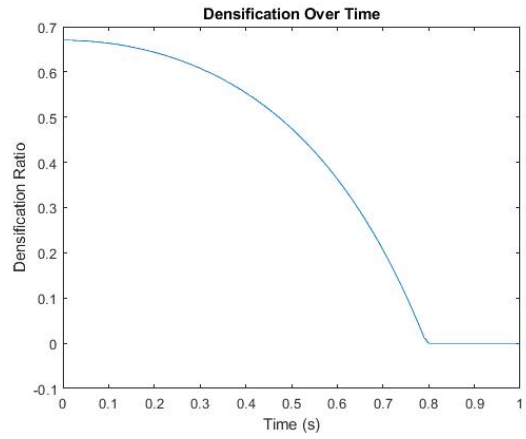
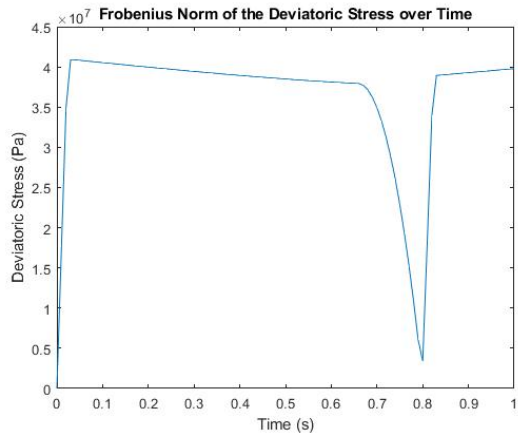
Densification decreases exponentially over time before full densification occurs around the 0.8 second mark, after which densification goes to zero. The temperature over time reaches a peak at roughly 800K near the time $t=0.65$. Note that the maximum temperature occurs just before complete solidification. This makes sense because we would not expect for the particulates to completely solidify at the maximum temperature. We expect the highest temperature in the middle of the stock material, after which it would propagate outwards.

This point represents the "sintering" where the particles are effectively binding together in their plastic state. This point is associated with the magnitude of the deviatoric Stress, which steadily drops off at $t=0.65$ (before solidification). After solidification ($t=0.8$), we see a sharp increase in the magnitude of the deviatoric stress, which is well evident because the particles have become completely solidified. The maximum of the 2-norm of the plastic strain over time should occur near the same mark as the zone of sintering. After solidification, we expect the plastic strain to go to zero.

Process Optimization Analysis

From the top 4 system parameters, there is some variation between the input parameters. Generally, the desired densification parameter falls within 0.539 ± 0.032 . The lowest cost value is for design 1, in which the J value was roughly $0.104 * 10^6 \frac{A}{m^2}$ larger than design 2 and yielded an 28.75 % lower II cost. Analyzing the densification parameters: 0.551 and 0.526, indicates that a larger current density has a greater affect on reaching the maximum temperature than an increase of the initial densification parameter.

DESIGN	D	J*10 ⁶	II
1	0.551	0.1961	0.0004
2	0.572	0.0925	0.0119
3	0.526	0.0714	0.0059
4	0.507	0.1837	0.0011

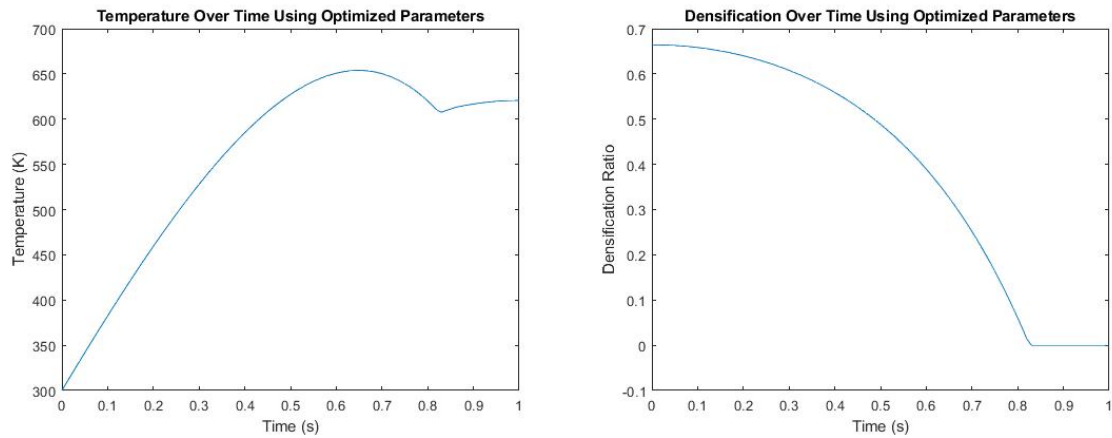


Further analysis to assert this claim could involve holding D constant, while varying J for several iterations to determine whether a minimum is achieved for higher values of J. Conversely, holding J constant while D is optimized could help determine the percentage reduction in cost. There are some limitations to this study, for example, in a commercial application, it would be important to run several design iterations, with broad ranges of D and J to apply the precise process parameters.

An important note from the analysis is to ensure that the cost function returns positive values (it was possible for it to return negative values if the densification parameter was set too low. This is a simple fix (simply new Π values).

Comparing the results with a classmate's, there are slight deviations in the cost for the best performer. Their cost values were extremely low (on the order of $5 * 10^{-7}$ to 0.0270). This difference could be from the result of the GA optimization and the number of generations it took to reach the desired value. It may also be due to minimum spikes, where a random value generated just happens to be extremely low, but is not populated enough to generate children that bring down the average. However, across the spectrum, the cost function is minimized for higher magnitudes of current density.

The graphs for temperature and densification over time using the optimized D and J parameters are shown below. While the curves look similar, the maximum temperature is much lower than without optimization, though densification occurs at the same time.



4 Conclusion

This report studied the compaction and sintering process in which a current is applied to a compressed stock material. Maximum temperatures and time of densification were determined from a process simulation in MATLAB, and a Genetic Algorithm was implemented to minimize the cost function varying two initial process parameters, namely the magnitude of current density and initial densification parameter..

An increase in the magnitude of the current density has a greater affect on meeting the maximum temperature than an increase in the initial densification parameter. This correlation makes sense in theory and practice, because the the final equation for the rate of thermal energy storage is independent of the mechanical energy, whereas the parameter d is small in the numerator.

Future Industry Applications

There are several areas to expand this report into commercial technology applications. Some example include manufacturing of complex additive manufacturing techniques such as SLA, FDM, and CAL, manufacturing of aerospace components such as turbine fan blades or high fidelity optical instruments for use on space systems, and optimizing the tolerance of certain subtractive manufacturing techniques to achieve a high degree of tolerance (as is useful in the semiconductor industry and commercial technology products).